Matrix Fixed Charge Density Modulates Exudate Concentration during Cartilage Compression

Lok Shun Ko and Thomas M. Quinn*

Department of Chemical Engineering, McGill University, Montreal, Quebec, Canada

ABSTRACT Electrolyte filtration arises due to the presence of fixed charges in cartilage extracellular matrix glycosaminoglycans (GAGs). Commonly assumed negligible, it can be important for design and interpretation of streaming potential measurements and modeling assumptions. To quantify the scale of this phenomenon, chloride ion concentration in exudate of compressed cartilage was measured by Mohr's titration and explant GAG content was colorimetrically assayed. Pilot studies indicated that an appropriate strain rate for experiments was 8×10^{-3} s^{-1} to eliminate concerns of exudate evaporation and explant damage (at low and high strain rates, respectively). Exudate chloride concentration of explants equilibrated in 1× PBS was significantly ($p < 0.05$) lower than the bath chloride concentration at strains of 37.5, 50, and 62.5%, with clear dependence on strain magnitude. Exudate chloride concentration was also significantly lower than that of the bath when 50% strain was applied after equilibration in 0.5, 1, and 2× PBS, with a trend for an increase in this relative difference with decreasing bath concentration ($p = 0.065$ between 0.5 and 2× PBS). Decreasing exudate chloride concentration correlated negatively with increasing postcompression GAG concentration. No difference between exudate chloride concentration and bath chloride concentration was ever observed for compression of uncharged agarose gel controls. Findings show that exudate from compressed cartilage is dilute relative to the bath due to the presence of matrix fixed charges, and this difference can generate diffusion potentials external to the explant, which may affect streaming potential measurements particularly under conditions of low strain rates and high strains.

INTRODUCTION

Articular cartilage is composed primarily of an extracellular matrix that is particularly rich in collagen type II and aggrecan. Aggrecan is comprised of glycosaminoglycans (GAGs) which bear a large number of negative fixed charges (1). These charges contribute to the strongly hydrophilic nature of GAGs, causing the osmotic swelling pressure that provides cartilage with its efficient load-bearing properties (2–4). The fixed charges on GAGs also give rise to electrostatic and electrokinetic phenomena which contribute importantly to tissue mechanical stiffness (5,6), hydraulic permeability (7,8), and streaming potentials (9–21). These properties can be valuable indicators of cartilage health and function (22,23) because they reflect the integrity of the extracellular matrix.

The loss of GAG is an important early marker of cartilage degradation, detectable before the signs are visible (24–26). Direct imaging of extracellular matrix composition is possible using modern clinical imaging methods (27,28), but high resolution localization of cartilage lesions and joint surface mapping of tissue integrity remains difficult. Handheld probes for arthroscopic assessment of cartilage mechanical (29) and electrokinetic (23,30,31) properties have therefore been developed in an effort to provide more quantitative diagnostic tools. These efforts are supported by a thorough understanding of the physical origins of the quantities measured. For the particular case of electrokinetic phenomena, this understanding is particularly challenging because of geometrical complexities (i.e., spatial dependence of fixed charge density, loading configuration, placement of electrodes) and due to coupling of measured signals (e.g., streaming potentials) with other phenomena such as fluid flows and matrix deformations.

A sometimes-overlooked phenomenon in the context of electrokinetic characterization of cartilage is that of electrolyte filtration (32): when a fluid flow is imposed through a charged membrane or tissue, the fluid flowing out (the exudate) is expected to have lower salt concentration than the bath. This phenomenon is often assumed negligible in experimental designs (13–17) and theoretical models (13,33); however, this oversight can lead to important errors and misinterpretations. For example, electrodes not placed directly against cartilage surfaces during streaming potential measurements may also measure the diffusion potential created by the difference in concentration between exudate and the surrounding bath caused by electrolyte filtration during cartilage compression. In addition, modeling of cartilage compression using an assumption that exudate has the same salt concentration as that of the bath can lead to erroneous conclusions regarding phenomena elsewhere in the tissue.

Our goals were therefore to more thoroughly characterize the phenomena of electrolyte filtration and reduced salt concentration of exudate as they apply to articular cartilage compression. Specifically, we aimed to measure chloride ion concentrations in the exudate of compressed cartilage,

Submitted August 13, 2012, and accepted for publication December 17, 2012.

*Correspondence: thomas.quinn@mcgill.ca

Editor: Peter Hunter.

0006-3495/13/02/0943/8 $2.00

http://dx.doi.org/10.1016/j.bpj.2012.12.036

to characterize the scale of this effect in relation to applied strains and matrix GAG concentrations (fixed charge densities), and to assess its relative importance in streaming potential measurements and theoretical models.

METHODS

Cartilage explants and agarose controls

Adult bovine knees were obtained from a local slaughterhouse and dissected to expose the distal femur. Osteochondral cores of 1-cm diameter were drilled perpendicular to the articular surface with a power drill and coring bit (model No. 05J05.50; Veritas Tools, Ottawa, Canada). Cores were placed in phosphate-buffered saline (PBS, cat. No. P5368; Sigma, St. Louis, MO) containing no Ca^{2+} nor Mg^{2+} at 0.5×, 1×, or 2× concentration and stored frozen at –20°C until experimental use. Bath pH was measured to be between 7.2 and 7.5 for all three concentrations used. After thawing, 100–200 μm of superficial tissue was removed with a microtome (model No. RM2235; Leica, Wetzlar, Germany) and a 1000-μm-thick cartilage sheet was cut. These sheets were then soaked in PBS of 0.5×, 1×, or 2× concentration for at least 40 min. Disks of 3-mm diameter were acquired from these sheets with a biopsy punch (model No. 33-32-P/25; Miltex, Integra Life Sciences, Plainsboro, NJ) immediately before mounting in a compression apparatus (below).

As control, sheets of 9.2% w/v agarose gel were prepared by adding 25 mL of 0.5×, 1×, or 2× PBS to 2.3 g agarose powder (cat. No. AGA002; BioShop Canada, http://www.bioshopcanada.com/info.asp) in a glass bottle. The bottle was then heated in a microwave and stirred every 10 s until the mixture was homogenous. This mixture was then cast between glass slabs (10 cm × 10 cm) at 1000-μm thickness and cooled at room temperature for 30 min. The gel was then transferred to a 0.5×, 1×, or 2× PBS bath and stored at 4°C until experimental use. Disks of 3-mm diameter were punched from the gel immediately before mounting in a compression apparatus (below).

Compression and exudate collection

Cartilage explant and agarose gel control disks were placed in a stainless-steel confined compression chamber (Fig. 1) mounted within a materials testing apparatus. A 3-mm diameter disk of filter paper (cat. No. 09-003-5E; Fisherbrand, Fisher Scientific, Loughborough, UK) was placed under the explant to aid fluid flow and to prevent bulging of the sample into the outflow hole. A displacement actuator was used to decrease explant thickness at constant strain rate while a load cell continuously recorded applied force. Exudate from the compressed tissue or gel sample flowed through the filter paper and into a 390-μm diameter hole beneath the sample and into a collection area. To prevent evaporation, a piece of cotton soaked in deionized water was placed immediately beneath the collection area, and a 100-mL humidifying water bath was placed next to the compression chamber (Fig. 1). The compression chamber, humidifying water bath, and compression hardware were all enclosed within a Plexiglas box. Once full compression was applied to samples, exudate (roughly 1 μL in total) was collected manually with a 10-μL pipettor (cat. No. 89130-554; VWR, Radnor, PA) and transferred to a 200-μL polymerase chain reaction (PCR) vial at which point titration (discussed below) was performed immediately. After titration of the exudate, the explant was removed from the apparatus and stored in another vial filled with 200 μL of 0.5×, 1×, or 2× PBS and frozen at –20°C until wet weight measurement (below). Only a single compression protocol was applied to any individual explant.

Reagent preparation and titration

Chloride concentration was determined by Mohr's titration (34). Silver nitrate was added to exudate until chloride ions were depleted by the formation of a white AgCl precipitate, at which point a potassium chromate indicator reacted with excess silver nitrate to form silver chromate, a red precipitate. Potassium chromate (K_2CrO_4) indicator solution (5% w/v) was prepared by adding 50 mg of potassium chromate (cat. No. SC-203351; Santa Cruz Biotechnology, Santa Cruz, CA) to 10 mL deionized water. The solution was filtered the next day to remove precipitates. Silver nitrate ($AgNO_3$) titrant (0.0705 M) was prepared by adding 0.5988 g of silver nitrate (cat. No. SC-203378; Santa Cruz Biotechnology) powder to 50-mL deionized water. Before the start of experiments, two 0.5-μL bath samples of known concentration were titrated, one fully and one partially (roughly 90%), to provide a guide for visual determination of titration endpoints.

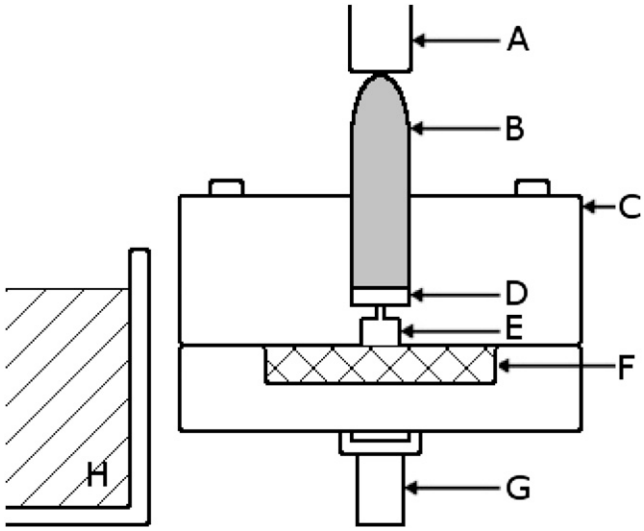

FIGURE 1 Schematic diagram of apparatus for tissue compression and exudate collection. (*A*) Loading post attached to load cell. (*B*) Stainless steel piston. (*C*) Stainless-steel confined compression chamber. (*D*) Cartilage explant over filter paper. (*E*) Exudate collection chamber. (*F*) Cotton soaked in deionized water (to prevent evaporation of exudate). (*G*) Support post to displacement actuator. (*H*) Deionized water bath (to prevent evaporation).

While explants were being compressed, 0.5 μL of K_2CrO_4 was added to a PCR vial and weighed on an analytical balance (model No. AL204; Mettler-Toledo, Columbus, OH). Once exudate was collected, 0.5 μL was transferred from the collection vial to the weighed PCR vial containing potassium chromate and the vial was weighed again to verify the amount of exudate added. Exudate was then titrated by first adding 3.5, 7, or 14 μL of silver nitrate solution depending on the relevant bath concentration of 0.5×, 1×, or 2× PBS, respectively. The remainder of the titration was then carried out by adding silver nitrate solution in 0.2-μL increments and stirring until the solution turned slightly orange and remained orange despite stirring. The vial was then weighed and the amount of titrant added was calculated by subtracting the pretitration weight from the final weight.

Wet weight, dry weight, and GAG content

Compressed explants were thawed for 60 min, superficial fluid was removed with a tissue, and wet weight was measured using an analytical balance. They were then lyophilized (FreeZone 2.5; Labconco, Kansas City, MO) overnight for dry weight measurement. Fluid content was calculated as the difference between wet and dry weights. Fluid volume fraction of explants was estimated from wet and dry weights assuming equal densities of solid and fluid matrix components. Each lyophilized explant was then digested overnight at 60°C in a vial containing 1 mL 1× PBS with 0.01% sodium azide, 5 mM cysteine-HCl, and 125 μg/mL papain (Sigma).

Explant GAG content was then colorimetrically assayed in a plate reader (model No. LB 940; Mithras, Berthold Technologies, Oak Ridge, TN) as previously described in Farndale et al. (35). Briefly, the digest solution was diluted ninefold with 1× PBS and 25 μL were mixed with 200 μL of dimethylmethylene-blue dye in a 96 well plate. Absorbance at 525 nm was then measured in the plate reader. Matrix GAG concentration was determined as micrograms of chondroitin sulfate per volume of matrix water (assuming a density of 1 mg/mL).

Experimental conditions

Three experimental protocols were developed to characterize our apparatus and the modulation of exudate concentration by matrix fixed charge density:

In the first protocol, 50% strain was applied at different strain rates to assess effects of evaporation. Various strain rates between 1.9×10^{-4} and 0.03 s^{-1} were applied to samples equilibrated in 1× PBS in the presence and absence of the damp cotton. Once experimental conditions were identified where cartilage mechanical failure and exudate evaporation were not problematic, protocols were developed to assess effects of bath ionic-strength and matrix fixed-charge density on exudate chloride concentration.

In the second protocol, strain was applied to samples equilibrated in 1× PBS at a rate of 8×10^{-3} s^{-1} to a range of maximum strains including 37.5, 50, and 62.5% to manipulate matrix fixed charge densities.

In the third protocol, 50% strain was applied at a rate of 8×10^{-3} s^{-1} to samples which were equilibrated in dilute (0.5×) and concentrated (2×) as well as regular (1×) PBS.

Statistical analysis

Significant ($p < 0.05$) differences in exudate chloride concentrations between samples compressed to different strain magnitudes were identified by analysis of variance and Tukey post hoc tests. Significant differences in concentration among baths, cartilage exudates, and control agarose exudates at various bath ionic strengths were identified similarly. Monotonic trends for exudate concentration versus explant fixed charge density were identified by linear least-square fits. Ninety-five-percent confidence interval lines were obtained on the basis of the t-distribution.

Theoretical estimate of exudate concentration

Anticipated exudate concentration was estimated from Donnan theory and species balance. Assuming uniform fixed charge density within homogeneous tissue specimens bathed in PBS where the dominant ions (Na^+ and Cl^-) are both monovalent, and assuming that steric exclusion of ions can be neglected, the intratissue concentrations of mobile ions (c_+ and c_-) are given by Grodzinsky (2) as

$$c_{\pm} = c_b e^{\mp \frac{F\Phi_D}{RT}}, \tag{1}$$

where c_b is the external bath concentration, F is Faraday's constant, Φ_D is the intratissue Donnan potential, R is the ideal gas constant, and T is absolute temperature. Intratissue ion concentrations are defined in terms of the intratissue water volume (V_f). Matrix fixed charge density ρ_m is expressed as Coulombs per volume of intratissue water, and is related to the Donnan potential through the electroneutrality condition

$$\rho_m = F(c_- - c_+) = 2Fc_b \sinh\left(\frac{F\Phi_D}{RT}\right). \tag{2}$$

During compression, we assume approximately uniform deformation of the tissue and conservation of fixed charge so that

$$\rho_{m,\text{final}} = \rho_{m,\text{initial}} * \frac{V_{f,\text{ initial}}}{V_{f,\text{ final}}}. \tag{3}$$

Similarly, intratissue mobile ion concentrations must be related to ion concentration in the exudate (c_e) by the species balances

$$c_{\pm,\text{initial}} * V_{f,\text{initial}} = c_{\pm,\text{final}} * V_{f,\text{final}} + c_e\left[V_{f,\text{initial}} - V_{f,\text{final}}\right]. \tag{4}$$

Therefore, determination of ρ_m and intratissue fluid volume before compression, and specification of compression amplitude, are sufficient to determine the change in fixed charge density from Eq. 3. Intratissue ion concentrations before and after compression can then be determined from fixed charge density using Eqs. 1 and 2, which then enables determination of exudate concentration from Eq. 4. It is important to note that this calculation provides an estimate of the average exudate concentration, given a finite increase in compressive strain from an initial state, rather than the concentration of exudate at the instant at which it flows out of the tissue.

As an illustration, a value of $\rho_m/F = 0.2$ mEq/mL was used together with an assumption of 80% fluid volume fraction to highlight the anticipated effects of compressive strain and bath ionic strength on exudate concentration (Fig. 2). As expected on physical grounds, exudate concentration is always less than bath concentration, with a difference that increases with increasing strain (increasing fixed charge density) and decreasing bath concentration.

RESULTS

Identification of appropriate strain rates

Initial studies focused on apparatus validation and testing, and the identification of an optimal range of strain rates. High strain rates can be associated with large loading forces and cartilage injury, while low strain rates can require long experiment durations leading to evaporation of exudate and inaccurate measurement of concentration. For compression of cartilage explants equilibrated in 1× PBS to 50% strain, no effect on exudate chloride concentration was

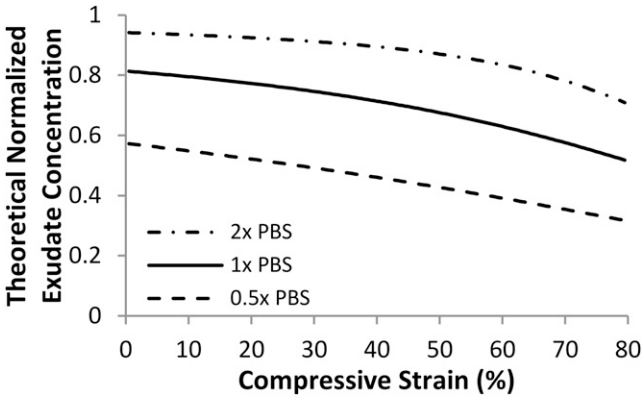

FIGURE 2 Theoretical calculation of exudate concentration versus compressive strain assuming initial values of $\rho m/F = 0.2$ mEq/mL and 80% fluid volume fraction. Calculations were performed for a range of different bath concentrations, and exudate concentration was normalized to bath concentration in each case.

observed for relatively high strain rates ranging from 3 to 30 $\times$ 10^{-3} s^{-1} (Fig. 3), provided that the damp cotton beneath the exudate collection chamber was present in the apparatus. However, at lower strain rates of 0.19–0.75 $\times$ 10^{-3} s^{-1}, exudate chloride concentration was measured to be higher than at higher strain rates and appeared to increase with decreasing strain rate (Fig. 3). This indicated that for the longer experimental durations associated with lower strain rates, evaporation of the exudate as it awaited collection was significant. Another set of experiments was carried out to further characterize these effects, wherein the damp cotton was absent. At 30 $\times$ 10^{-3} s^{-1}, the measured exudate chloride concentration was comparable to that obtained in experiments where the damp cotton was present. However, measured exudate chloride concentrations at smaller strain rates of 0.75 and 3 $\times$ 10^{-3} s^{-1} were markedly elevated with respect to measurements where the damp cotton was present, indicative of more rapid evaporation (Fig. 3). Based on these measurements, and considering that 30 $\times$ 10^{-3} s^{-1} strain rate involved loads which nearly exceeded the capacity of our apparatus, we adopted a strain rate of 8 $\times$ 10^{-3} s^{-1} for use in all subsequent experiments.

Magnitude of strain and bath ionic strength affect cartilage exudate chloride concentration

For cartilage explants equilibrated in 1$\times$ PBS, compression to 37.5, 50, and 62.5% strain all resulted in exudate chloride concentrations which were significantly less than that of the bath (Fig. 4 *A*). Furthermore, exudate chloride concentration decreased as total strain increased: for 62.5% strain, it was significantly lower than for 37.5% strain. For cartilage explants compressed to 50% strain after equilibration with

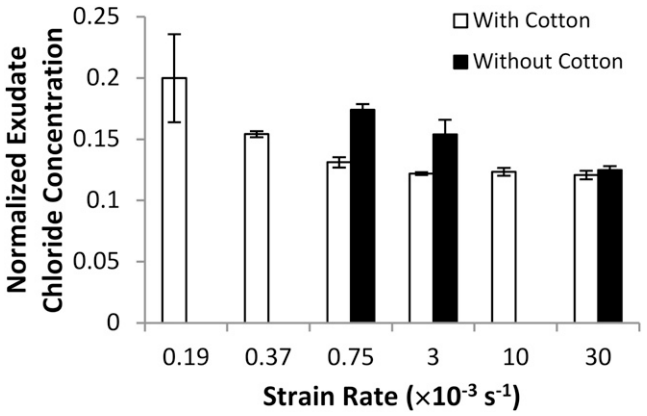

FIGURE 3 Exudate concentration as measured after compression at different strain rates. Explants were compressed by 50% in the presence or absence of a damp piece of cotton within the compression apparatus. With the damp cotton in place, at strain rates below 3 $\times$ 10^{-3} s^{-1} (relatively long experimental durations), exudate concentration was greater than that measured at higher strain rates, suggesting possible evaporation. Without the damp cotton, this transition appeared to happen at somewhat higher strain rates (even shorter durations). Mean $\pm$ SE ($n = 5$).

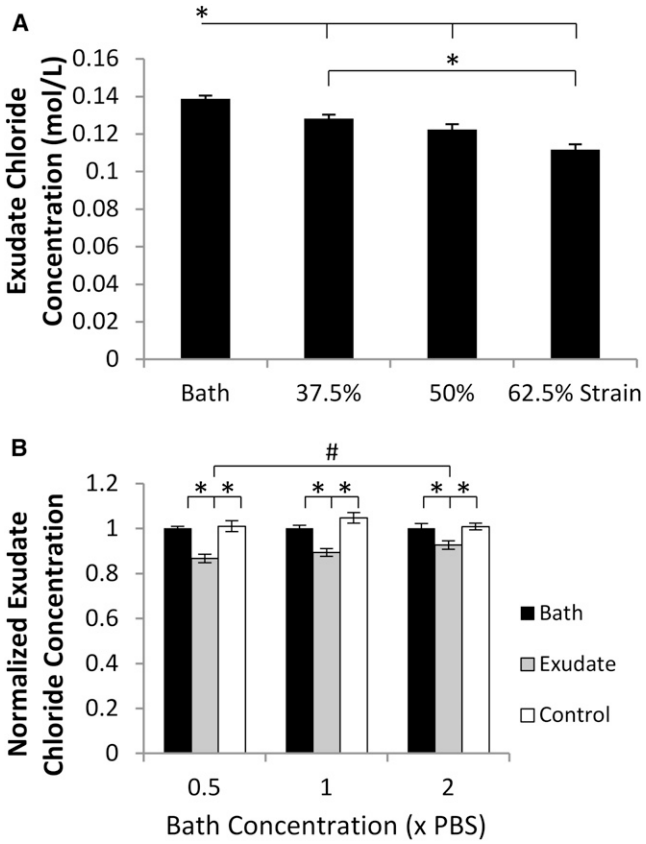

FIGURE 4 Cartilage exudate concentration measured versus compressive strain amplitude and changing bath concentration. (*A*) Bath and exudate concentrations versus magnitude of compressive strain, for tissue samples in a bath of 1$\times$ PBS (0.14 M NaCl). Mean $\pm$ SE ($n = 8$); the asterisk represents $p < 0.05$. (*B*) Exudate concentration normalized to bath concentration for bath concentrations of 0.5$\times$, 1$\times$, and 2$\times$ PBS. Bath concentrations were compared to exudates from cartilage and uncharged agarose gels (controls). Mean $\pm$ SE ($n = 8$); asterisk represents $p < 0.05$; pound sign represents $p = 0.065$.

baths of 0.5$\times$, 1$\times$, and 2$\times$ PBS, exudate chloride concentration was always significantly less than that of the bath (Fig. 4 *B*). In addition, control exudates generated by compression of agarose gels equilibrated in the same baths were equivalent to bath concentrations and always greater than cartilage exudates. For cartilage explants, there was also an evident trend toward lower normalized exudate chloride concentrations for lower bath ionic strength. In other words, the reduction in exudate chloride concentration below that of the bath was more dramatic for lower bath ionic strengths; this trend approached significance at $p = 0.065$ (Fig. 4 *B*).

Cartilage exudate chloride concentration correlates negatively with matrix GAG concentration

For cartilage explants equilibrated in 1$\times$ PBS and compressed to 37.5, 50, and 62.5% strain, exudate chloride

concentration tended to decrease with increasing precompression matrix GAG concentration (Fig. 5, *A–C*). In all of these cases, regression best-fit lines had negative slopes; however, the upper 95% confidence interval best-fit line had positive slope, indicating trends as opposed to significant findings. When exudate chloride concentration was considered versus postcompression matrix GAG concentration, for all three levels of applied strain taken together, exudate chloride concentration decreased with increasing final GAG concentration (Fig. 5 *D*). This finding was significant, with the upper bound of the 95% confidence interval also exhibiting negative slope (Fig. 5 *D*).

DISCUSSION

Measurements of chloride concentration in exudate of compressed articular cartilage clearly demonstrated the effects of applied strain and bath ionic strength on exudate concentration, consistent with theoretical expectations. For cartilage explants, exudate chloride concentration was always lower than bath chloride concentration for the range of bath concentrations from 0.5 to 2× PBS. In the absence of matrix fixed charges, as was the case for agarose gel controls (36), exudate chloride concentration remained at bath concentration under identical conditions. Increasing strain was associated with increasingly dramatic differences between exudate and bath chloride concentrations, as expected due to increased fix charge density with tissue compression. This correlation between exudate chloride concentration and postcompression explant GAG concentration was found to be statistically significant. Also consistent with theoretical expectations, the relative difference between exudate and bath salt concentrations increased with decreasing bath ionic strength. These effects, reminiscent of reverse osmosis for flows of salt solutions through charged membranes, arise due to fixed charges within the cartilage extracellular matrix and are straightforwardly interpreted using classical electrokinetic theory.

Previous modeling work by Bathe et al. (37) has shown that, at physiological pH, chondroitin and chondroitin-4-sulfate are essentially fully ionized in the relevant range of bath ionic strength. Assuming that all chondroitin sulfate groups are fully ionized and that each carries two negative charges (12), measured matrix GAG concentration can be translated into an expected fixed charge density (FCD) for the cartilage samples studied. Using Eqs. 1–4, this can be used to predict the expected changes in exudate concentration from matrix GAG concentration. Surprisingly, this calculation leads to the conclusion that the fixed charge density required to produce the exudate concentrations observed in this study was roughly seven times higher than the fixed charge density determined from GAG measurements. Some of this discrepancy may have been due to the presence of other charged groups within the extracellular matrix, such as keratan sulfate. Another partial explanation may be associated with water partitioning in cartilage: intrafibrillar fluid, which hydrates the collagen matrix, may be less mobile during cartilage compression than extrafibrillar fluid, which interacts more with GAGs, resulting in a higher effective FCD (38). However, neither of these phenomena is expected to account for the factor of seven in the discrepancy observed.

The bulk of this discrepancy between theory and measurements is likely due to the inaccuracy of our simplifying assumption of matrix homogeneity during tissue compression. Equations 1–4 are valid for homogeneous regions of tissue and can only be expected to apply over an entire explant during compression if deformations are applied more slowly than the gel diffusion rate (39). Localized areas of high compressive strain are created near sites of fluid exudation from more rapidly (as in this study) compressed cartilage, especially during confined compression

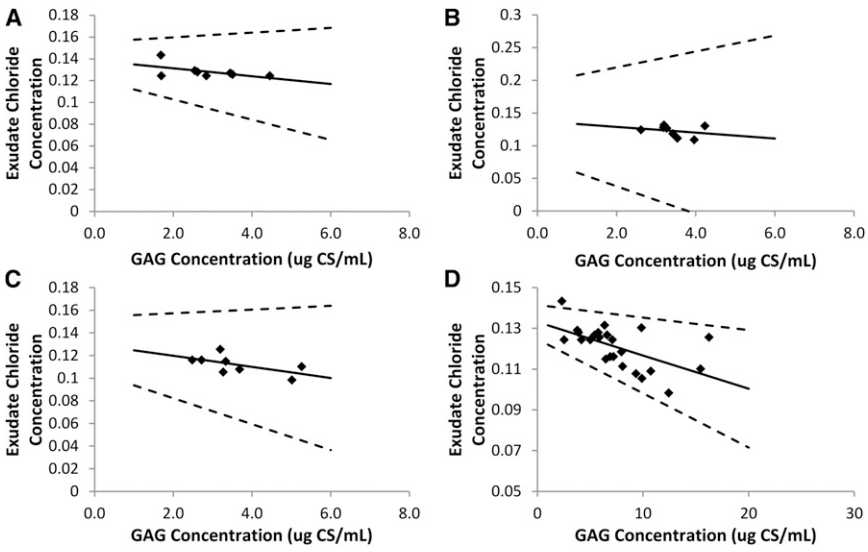

FIGURE 5 Cartilage exudate concentrations versus individual explant GAG concentrations before and after compression, for samples in 1× PBS. Exudate concentration for (*A*) 37.5%, (*B*) 50%, and (*C*) 62.5% compressive strain versus explant GAG concentrations before compression. (*D*) Exudate concentration for 37.5, 50, and 62.5% compressive strain versus explant GAG concentrations after compression. (*Solid lines*) Linear regression best fits. (*Dotted lines*) 95% confidence intervals for regression best fits.

(7). In our study, this would have occurred near to the hole through which exudate flowed, creating a zone of relatively high fixed charge density which would strongly influence the concentration of exudate. Presumably, our compression experiments therefore involved matrix strains near the outflow region several times greater than those in the tissue bulk. This phenomenon may provide a means for assaying local strains during cartilage compression, and its associated insights may complement previous theoretical work exploring the origins of diffusion potentials in compressed cartilage (40).

The presence of relatively dilute exudate indicates that a diffusion boundary layer arises in the vicinity of compressed cartilage, at interfaces with a surrounding bath where fluid outflow occurs. By analogy with reverse osmosis, similar effects should also be expected at interfaces where fluid inflow occurs, due to increased concentration of bath ions in those areas. If a diffusion boundary layer is located between measurement electrodes, a diffusion potential may interfere with measurement of streaming potential. To estimate the scale of this error, consider a typical one-dimensional confined compression experiment where an explant of thickness d is subject to a compression velocity U against a rigid, insulating porous platen by an impermeable electrode, with a second electrode downstream of the platen. Assuming that the exudate is at uniform concentration and that mixing between the exudate and the sodium chloride bath is due to diffusion only, a potential difference between the exudate and the bath (ϕ_d) will be generated of magnitude (41)

$$\Phi_d = 0.2\frac{RT}{F}\ln\left(\frac{C_b}{C_e}\right). \tag{5}$$

Within the tissue, the streaming potential (ϕ_u) is estimated from equations of mobile ion flux dominated by advection and migration as

$$\Gamma_\pm = Uc_\pm \mp u_\pm c_\pm \nabla\varphi_u, \tag{6}$$

where the $u_\pm$ values are the ion electrical motilities. Combining Eq. 6 with constraints of electroneutrality and zero current (open circuit) provides the estimate

$$\Phi_u = \left(\frac{c_+ - c_-}{u_+c_+ + u_-c_-}\right)Ud. \tag{7}$$

The ratio between the anticipated diffusion potential external to a compressed cartilage explant and the associated streaming potential may therefore be written as

$$\frac{\Phi_d}{\Phi_u} = \frac{0.2\sigma\frac{RT}{F}\ln\left(\frac{C_b}{C_e}\right)}{\rho_m Ud}, \tag{8}$$

where σ represents the conductivity of saline inside the tissue.

For a sodium chloride bath at physiological concentration (0.14 M), a fixed charge density of 0.10 mEq/mL (corresponding to the FCD required to produce measured exudate concentrations in this study), a fluid volume fraction of 0.8, and an explant thickness of 500 μm, Eqs. 1–7 were used to estimate ϕ_d and ϕ_u. The two potentials and their ratio were compared as a function of strain, at a strain rate of 1.5×10^{-3} s^{-1} (Fig. 6 *A*). At low strains ϕ_d is relatively small compared to the streaming potential. At high strains of 60% and above, exudate concentration decreases due to increasing matrix FCD while streaming potential decreases due to decreasing thickness, allowing the diffusion potential to reach roughly 10% of the streaming potential. The same calculations were repeated for a strain of 50% and as a function of strain rate (Fig. 6 *B*). Because exudate concentration is independent of strain rate, ϕ_d is constant in this case. The streaming potential increases linearly as a function of strain rate so that ϕ_d is only relatively important at low strain rates, reaching 10% of the streaming potential at roughly 1×10^{-3} s^{-1}. Based on these estimates, it would seem

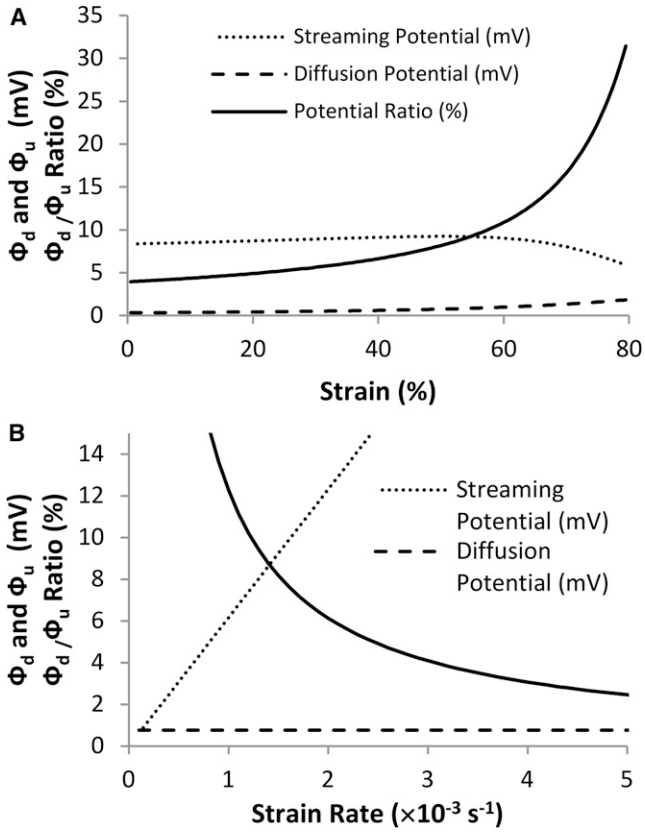

FIGURE 6 Theoretical comparison of the relative importance of the intratissue streaming potential and diffusion potentials, which would occur in the bath due to mixing with dilute exudate. (*A*) Theoretical estimates of the streaming potential (ϕ_u; *dotted line*), diffusion potential (ϕ_d; *dashed line*), and their ratio (ϕ_d/ϕ_u; *solid line*) as a function of strain given a strain rate of 1.5×10^{-3} s^{-1}. (*B*) Theoretical estimates of the streaming potential (*dotted line*), diffusion potential (*dashed line*), and their ratio (*solid line*) at 50% compression as a function of strain rate.

that diffusion potentials between exudate from compressed cartilage and surrounding baths can be significant compared to the streaming potential under conditions of low strain rates or high strains (when the product *Ud* is relatively small; see Eq. 8). Regardless, it is important to note that these effects will only confound measurements of streaming potential if a diffusion boundary layer appears between electrodes.

Relatively dilute exudate is also expected when fluid flow is imposed through cartilage or other charged matrices via a pressure difference. This effect is commonly known as reverse osmosis (42). Fixed charges in the extracellular matrix impede the flow of ions and zones of concentration polarization that form upstream and downstream of the matrix. Measurements of streaming potentials generated this way are therefore also affected by diffusion potentials, and as cautioned by Maroudas et al. (12):

> "It is important to take as the true value of the streaming potential the rise in the potential difference between the two electrodes obtained immediately upon the application of pressure, as continued flow results in the production of extraneous potentials due to electrolyte filtration."

There are several examples in the literature of streaming potential measurements where the effects of electrolyte filtration were not explicitly addressed but may have contributed to measured potentials due to placement of electrodes around a zone of concentration polarization (13–17,33). As described above, associated errors in these cases would likely have been minor; nevertheless, an interpretation of the potentials measured in these experiments as arising solely from the streaming potential generated within the bulk of the material studied must be regarded as approximate. Related issues may be pertinent to the interpretation of modeling work, which predicts the appearance of unbalanced charge at membrane interfaces despite the essentially instantaneous rate of charge relaxation in physiological saline (33). This modeling work is based upon the assumption that effects of electrolyte filtration are negligible such that ion fluxes are continuous across a charged membrane or tissue. We show here that this assumption is clearly not true for cartilage compression, and that electrolyte filtration is expected to contribute significantly to distributions of ions around tissues through which fluid flows.

Our results also highlight the possibility of using measurements of exudate chloride concentration as a means for nondestructive estimation of matrix fixed charge density. An evident limitation of this approach is the low volume of exudate which can be acquired from tissue compression. Greater precision would be obtained through titration of a larger quantity of exudate, thereby reducing the severity of overshoot. Precise collection of exudate is also difficult because some exudate tends to flow around the exterior of the specimen during compression. These technical challenges can likely be overcome, however, and these methods could provide a means for nondestructive characterization of fixed charge and matrix deformations (affecting fixed charge density) during tissue compression.

This work was supported by the Natural Sciences and Engineering Research Council of Canada's Discovery Grant and Research Chair Programs of Canada (to T.M.Q.) and by an Eugenie Ulmer Lamothe Graduate Fellowship (to L.S.K.).

REFERENCES

1. Rosenberg, L., W. Hellmann, and A. K. Kleinschmidt. 1970. Macromolecular models of protein polysaccharides from bovine nasal cartilage based on electron microscopic studies. *J. Biol. Chem.* 245:4123–4130.
2. Grodzinsky, A. J. 1983. Electromechanical and physicochemical properties of connective tissue. *Crit. Rev. Biomed. Eng.* 9:133–199.
3. Williamson, A. K., A. C. Chen, and R. L. Sah. 2001. Compressive properties and function-composition relationships of developing bovine articular cartilage. *J. Orthop. Res.* 19:1113–1121.
4. Chen, S. S., Y. H. Falcovitz, …, R. L. Sah. 2001. Depth-dependent compressive properties of normal aged human femoral head articular cartilage: relationship to fixed charge density. *Osteoarthritis Cartilage.* 9:561–569.
5. Buschmann, M. D., and A. J. Grodzinsky. 1995. A molecular model of proteoglycan-associated electrostatic forces in cartilage mechanics. *J. Biomech. Eng.* 117:179–192.
6. Quinn, T. M., P. Dierickx, and A. J. Grodzinsky. 2001. Glycosaminoglycan network geometry may contribute to anisotropic hydraulic permeability in cartilage under compression. *J. Biomech.* 34:1483–1490.
7. Chin, H. C., G. Khayat, and T. M. Quinn. 2011. Improved characterization of cartilage mechanical properties using a combination of stress relaxation and creep. *J. Biomech.* 44:198–201.
8. Reynaud, B., and T. M. Quinn. 2006. Anisotropic hydraulic permeability in compressed articular cartilage. *J. Biomech.* 39:131–137.
9. Lotke, P. A., J. Black, and S. Richardson. 1974. Electromechanical properties in human articular cartilage. *J. Bone Joint Surg. Am.* 56:1040–1046.
10. Légaré, A., M. Garon, …, M. D. Buschmann. 2002. Detection and analysis of cartilage degeneration by spatially resolved streaming potentials. *J. Orthop. Res.* 20:819–826.
11. Garon, M., A. Légaré, …, M. D. Buschmann. 2002. Streaming potentials maps are spatially resolved indicators of amplitude, frequency and ionic strength-dependent responses of articular cartilage to load. *J. Biomech.* 35:207–216.
12. Maroudas, A., H. Muir, and J. Wingham. 1969. The correlation of fixed negative charge with glycosaminoglycan content of human articular cartilage. *Biochim. Biophys. Acta.* 177:492–500.
13. Gu, W. Y., W. M. Lai, and V. C. Mow. 1993. Transport of fluid and ions through a porous-permeable charged-hydrated tissue, and streaming potential data on normal bovine articular cartilage. *J. Biomech.* 26:709–723.
14. Fujisaki, K., S. Tadano, and N. Asano. 2011. Relationship between streaming potential and compressive stress in bovine intervertebral tissue. *J. Biomech.* 44:2477–2481.
15. Frank, E. H., A. J. Grodzinsky, …, D. R. Eyre. 1987. Streaming potentials: a sensitive index of enzymatic degradation in articular cartilage. *J. Orthop. Res.* 5:497–508.
16. Frank, E. H., and A. J. Grodzinsky. 1987. Cartilage electromechanics—II. A continuum model of cartilage electrokinetics and correlation with experiments. *J. Biomech.* 20:629–639.

17. Chen, A. C., T. T. Nguyen, and R. L. Sah. 1997. Streaming potentials during the confined compression creep test of normal and proteoglycan-depleted cartilage. *Ann. Biomed. Eng.* 25:269–277.

18. Lee, R. C., E. H. Frank, …, D. K. Roylance. 1981. Oscillatory compressional behavior of articular cartilage and its associated electromechanical properties. *J. Biomech. Eng.* 103:280–292.

19. Grodzinsky, A. J., H. Lipshitz, and M. J. Glimcher. 1978. Electromechanical properties of articular cartilage during compression and stress relaxation. *Nature.* 275:448–450.

20. Kim, Y.-J., L. J. Bonassar, and A. J. Grodzinsky. 1995. The role of cartilage streaming potential, fluid flow and pressure in the stimulation of chondrocyte biosynthesis during dynamic compression. *J. Biomech.* 28:1055–1066.

21. Reynaud, B., and T. M. Quinn. 2006. Tensorial electrokinetics in articular cartilage. *Biophys. J.* 91:2349–2355.

22. Gu, W. Y., X. G. Mao, …, V. C. Mow. 1999. Streaming potential of human lumbar annulus fibrosus is anisotropic and affected by disc degeneration. *J. Biomech.* 32:1177–1182.

23. Changoor, A., J. P. Coutu, …, M. D. Buschmann. 2011. Streaming potential-based arthroscopic device is sensitive to cartilage changes immediately post-impact in an equine cartilage injury model. *J. Biomech. Eng.* 133:061005.

24. Maroudas, A. I. 1976. Balance between swelling pressure and collagen tension in normal and degenerate cartilage. *Nature.* 260:808–809.

25. Bonassar, L. J., K. A. Jeffries, …, A. J. Grodzinsky. 1995. Cartilage degradation and associated changes in biochemical and electromechanical properties. *Acta Orthop. Scand. Suppl.* 266:38–44.

26. Shet, K., S. M. Siddiqui, …, X. Li. 2012. High-resolution magic angle spinning NMR spectroscopy of human osteoarthritic cartilage. *NMR Biomed.* 25:538–544.

27. Kulmala, K. A., R. K. Korhonen, …, J. Töyräs. 2010. Diffusion coefficients of articular cartilage for different CT and MRI contrast agents. *Med. Eng. Phys.* 32:878–882.

28. Silvast, T. S., H. T. Kokkonen, …, J. Töyräs. 2009. Diffusion and near-equilibrium distribution of MRI and CT contrast agents in articular cartilage. *Phys. Med. Biol.* 54:6823–6836.

29. Virén, T., S. Saarakkala, …, J. Töyräs. 2011. Ultrasound evaluation of mechanical injury of bovine knee articular cartilage under arthroscopic control. *IEEE Trans. Ultrason. Ferroelectr. Freq. Control.* 58:148–155.

30. Quenneville, E., J. S. Binette, …, M. D. Buschmann. 2004. Fabrication and characterization of nonplanar microelectrode array circuits for use in arthroscopic diagnosis of cartilage diseases. *IEEE Trans. Biomed. Eng.* 51:2164–2173.

31. Berkenblit, S. I., E. H. Frank, …, A. J. Grodzinsky. 1994. Electrokinetic methods for arthroscopic detection of cartilage degeneration in synovial joints. *Annu. Int. Conf. IEEE Eng. Med. Biol. Soc.* 742: 746–747.

32. Starov, V. M., and N. V. Churaev. 1993. Separation of electrolyte solutions by reverse osmosis. *Adv. Colloid Interface Sci.* 43:145–167.

33. Quenneville, E., and M. D. Buschmann. 2005. A transport model of electrolyte convection through a charged membrane predicts generation of net charge at membrane/electrolyte interfaces. *J. Membr. Sci.* 265:60–73.

34. Hillebrand, W. F., and G. E. F. Lundell. 1955. Applied Inorganic Analysis, with Special Reference to the Analysis of Metals, Minerals, and Rocks. Wiley, New York.

35. Farndale, R. W., D. J. Buttle, and A. J. Barrett. 1986. Improved quantitation and discrimination of sulphated glycosaminoglycans by use of dimethylmethylene blue. *Biochim. Biophys. Acta.* 883:173–177.

36. Normand, V., D. L. Lootens, …, P. Aymard. 2000. New insight into agarose gel mechanical properties. *Biomacromolecules.* 1:730–738.

37. Bathe, M., G. C. Rutledge, …, B. Tidor. 2005. A coarse-grained molecular model for glycosaminoglycans: application to chondroitin, chondroitin sulfate, and hyaluronic acid. *Biophys. J.* 88:3870–3887.

38. Maroudas, A., E. Wachtel, …, P. Weinberg. 1991. The effect of osmotic and mechanical pressures on water partitioning in articular cartilage. *Biochim. Biophys. Acta.* 1073:285–294.

39. Morel, V., and T. M. Quinn. 2004. Cartilage injury by ramp compression near the gel diffusion rate. *J. Orthop. Res.* 22:145–151.

40. Lai, W. M., V. C. Mow, …, G. A. Ateshian. 2000. On the electric potentials inside a charged soft hydrated biological tissue: streaming potential versus diffusion potential. *J. Biomech. Eng.* 122:336–346.

41. Gorman, M., and S. M. C. Murphy. 1949. Liquid junction potential calculations. *J. Chem. Educ.* 26:579.

42. Bird, R. B., W. E. Stewart, and E. N. Lightfoot. 2007. Transport Phenomena. J. Wiley, New York.